

Supplement of The Cryosphere, 13, 1513–1528, 2019
<https://doi.org/10.5194/tc-13-1513-2019-supplement>
© Author(s) 2019. This work is distributed under
the Creative Commons Attribution 4.0 License.



Supplement of

Rapid retreat of permafrost coastline observed with aerial drone photogrammetry

Andrew M. Cunliffe et al.

Correspondence to: Andrew M. Cunliffe (a.cunliffe@exeter.ac.uk)

The copyright of individual parts of the supplement might differ from the CC BY 4.0 License.

Table S1. Processing parameters for photogrammetric reconstructions in Agisoft PhotoScan:

Step	Parameter	Value
Image quality assessment	Minimum quality score	≥0.7
Image alignment	Accuracy	Highest
	Generic preselection	Yes
	Reference preselection	Yes
	Key point limit	40,000
	Tie point limit	0
	Adaptive camera model fitting	No
Tie point filtering	Reprojection error threshold	0.45
Parameter optimisation	Enabled parameters:	F, Cz, Cy, B1, B2, K1, K2, K3, P1, P2
	Fit rolling shutter	No
Dense cloud (Multi-view stereopsis)	Quality	High
	Depth filtering	Mild
Orthomosaic	Mapping mode	Orthophoto
	Blending mode	Mosaic
	Enable colour correction	Yes
	Enable hole filling	Yes
Digital Surface Model (DSM)	Surface type	Height field
	Source data	Dense cloud
	Interpolation	Enabled
	Quality	High
	Depth filtering	Mild

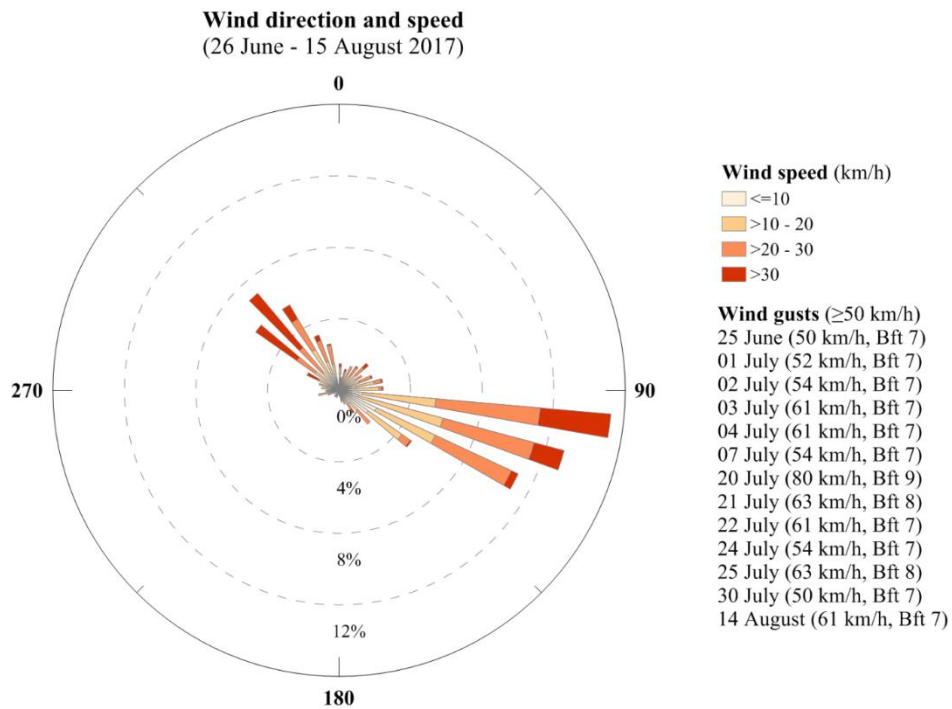


Figure S1. Wind direction, frequency and speed observed on Kuvluraq – Simpson Point, Qikiqtaruk - Herschel Island from 2017-06-16 to 2017-08-15. Three strong easterly wind events (>30 km/h wind speed) were observed during the observation period; Data source: Environment Canada 2017.

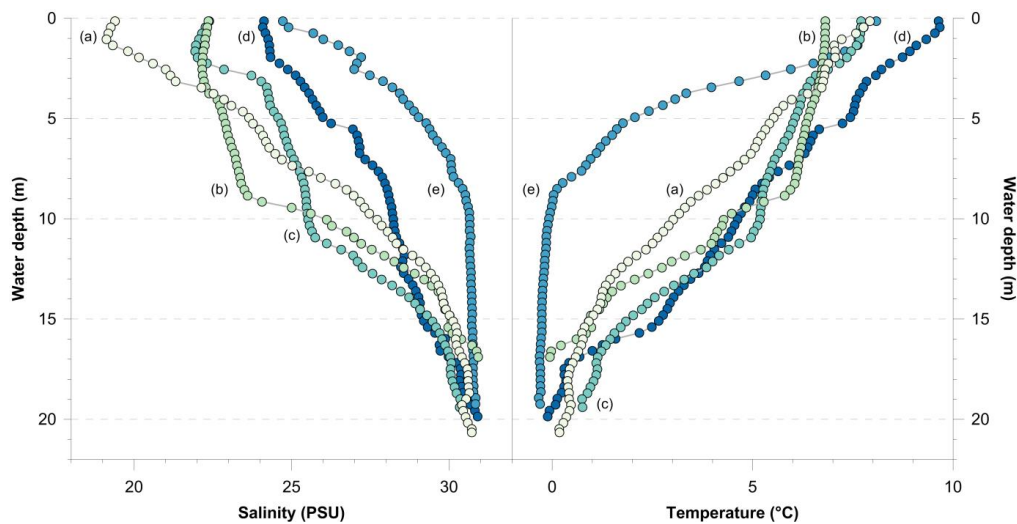


Figure S2. Seawater temperatures and salinity measured in close proximity to the land within 2 km of Kuvluraq – Simpson Point, made between 2017-07-21 and 2017-08-02; (a) 2017-07-21, (b) 2017-07-23, (c) 2017-07-25, (d) 2017-07-28, and (e) 2017-08-02.



Figure S3. Example of cliff erosion via block failure due to undercutting. The vegetated active layer (i.e. seasonally thawed part of the soil) has subsequently detached from the collapsed block.



Figure S4. Change in mean shoreline position for all time points, y-axis errors represent total shoreline uncertainty (Table 1). The solid line is a linear model, fitted by least squares, and has a slope of 1.94 ± 0.5 ($\text{m yr}^{-1}; \pm \text{SE}$).

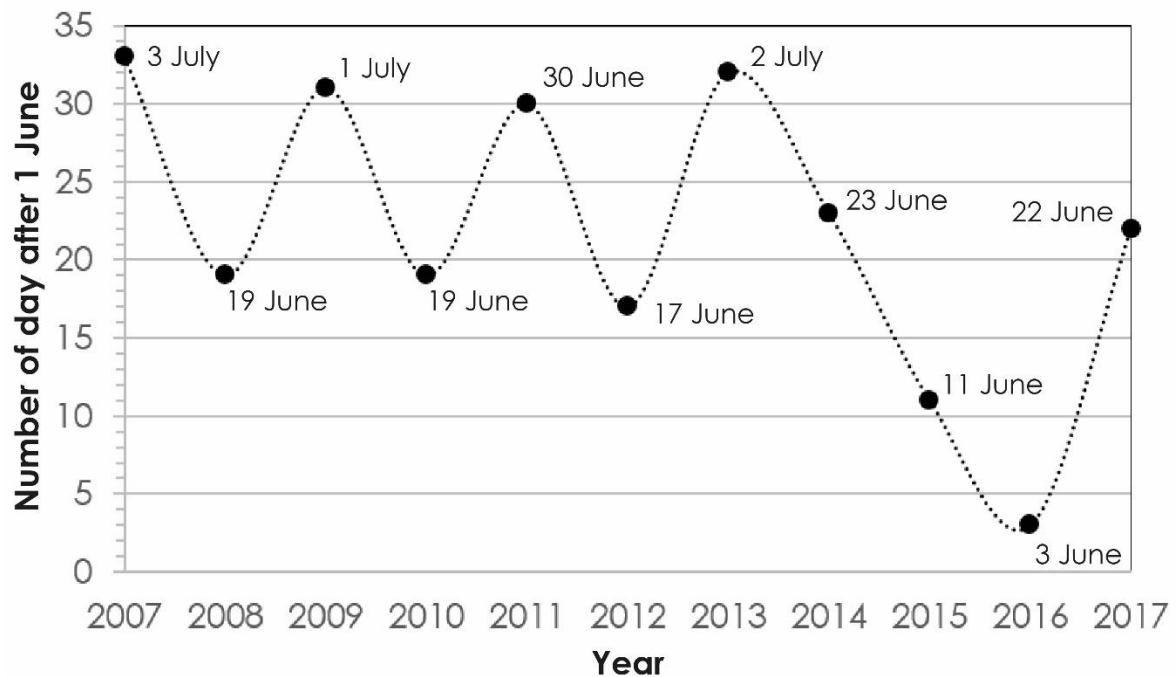


Figure S5. Start of the open water season, extracted from MODIS observations (Nasa WorldView, <https://worldview.earthdata.nasa.gov/>). The two years preceding 2017 experienced early than typical break up, but 2017 was in line with the decadal average.

Video S1. Created from hourly time-lapse images, looking west by southwest towards the Pauline Cove settlement from 69.570553°N, -138.880706°E, between 2017-07-29 and 2017-08-03. Available online at <https://doi.org/10.5446/40250>.

References:

- ESRI, Garmin, HERE, MapmyIndia, INCREMENT, OpenStreetMap, GIS Community, 2018. Basemap.
- Thompson, F., 1994. Illustrations from : An Interpretive Manual for Reports on Granular Deposits in the Inuvialuit Settlement Region : Part of the Inuvialuit Final Agreement Implementation Program, Task 7 - Sand and Gravel, Northern Affairs Program. Land Management. Indian and Northern Affairs Canada, Ottawa, Canada.
- Wessel, P., Smith, W.H.F., 1996. Shorelines: Wessel, Pål, and Walter H. F. Smith. "A Global, Self-Consistent, Hierarchical, High-Resolution Shoreline Database." *Journal of Geophysical Research: Solid Earth* 101, no. B4 (1996): 8741–8743. <https://doi.org/10.1029/96JB00104>. *Journal of Geophysical Research: Solid Earth* 101, 8741–8743. <https://doi.org/10.1029/96JB00104>